Title

Single protonation of the reduced quinone in respiratory complex I drives four-proton pumping

Journal

FEBS Letters, 597(2)

ISSN

0014-5793

Authors

Stuchebrukhov, Alexei A

Hayashi, Tomoyuki

Publication Date

2023

DOI

10.1002/1873-3468.14518

Peer reviewed

HHS Public Access

Author manuscript

FEBS Lett. Author manuscript; available in PMC 2024 January 01.

Published in final edited form as:

FEBS Lett. 2023 January ; 597(2): 237–245. doi:10.1002/1873-3468.14518.

Single protonation of the reduced quinone in respiratory complex I drives four-proton pumping

Alexei A. Stuchebrukhov[*],

Tomoyuki Hayashi

Department of Chemistry, University of California, Davis, CA 95616

Abstract

Complex I is a key proton-pumping enzyme in bacterial and mitochondrial respiratory electron transport chains. Using quantum chemistry and electrostatic calculations, we have examined the pKa of the reduced quinone QH-/QH2 in the catalytic cavity of complex I. We find that pKa(QH-/QH2) is very high, above 20. This means that the energy of a single protonation reaction of the doubly reduced quinone (i.e. the reduced semiquinone QH-) is sufficient to drive four protons across the membrane with a potential of 180mV. Based on these calculations, we propose a possible scheme of redox-linked proton pumping by complex I. The model explains how the energy of the protonation reaction can be divided equally between four pumping units of the pump, and how a single proton can drive translocation of four additional protons in multiple pumping blocks.

Graphical Abstract

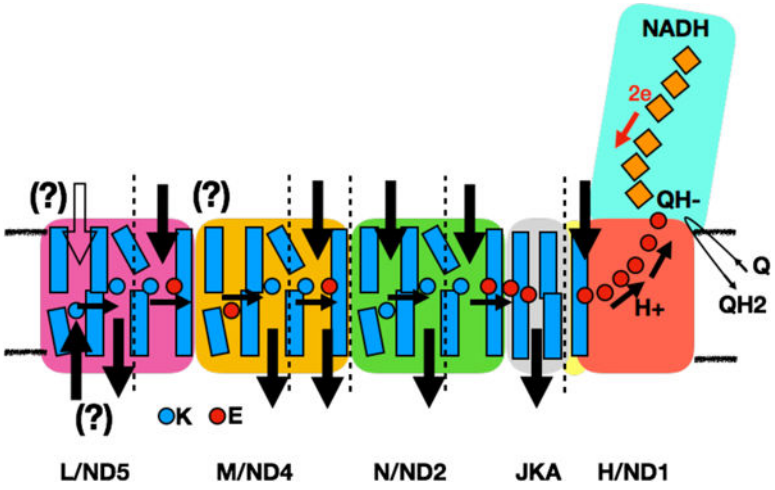

Complex I is a key proton-pumping enzyme in bacterial and mitochondrial respiratory electron transport chains. Quantum chemistry calculations suggest that the energy of a single protonation reaction of the reduced semiquinone QH- in the catalytic cavity of complex I is sufficient to drive four protons across the membrane. A novel scheme of redox-linked proton pumping by complex I is proposed.

[*]corresponding author, aastuchebrukhov@ucdavis.edu, Department of Chemistry, University of California, Davis, CA 95616.

Keywords

Mitochondria; respiratory complex I; NADH dehydrogenase; proton pumping; coupled electron-proton transfer; proton translocation

Introduction

Complex I is a key proton-pumping enzyme in bacterial and mitochondrial respiratory electron transport chains.[1–2] Recent structural studies[3–13] of the enzyme have revealed molecular details that suggest possible molecular mechanisms of its redox-driven 4H+/2e- proton pumping[14–16] across the membrane. Recently, a number of different models have been considered in the literature, see, e.g. Refs.[11, 14–20]; however, there is no consensus yet on the complete mechanism of complex I. The two-electron reduction of quinone[21–22] is a key exergonic step which provides energy for pumping four protons across the membrane; presumably, it occurs via local Coulomb and conformational changes[2, 11, 23] at the catalytic site that transmit to the membrane domain of the enzyme and generate proton pumping[24–25]. However, there is no yet clear understanding of how exactly the redox energy of quinone reduction is transformed into proton pumping, nor the redox chemistry at the catalytic site of the enzyme is well understood.

Here, on the basis of electronic structure and electrostatic calculations, we examine the pKa's and redox potentials of the first Q/QH and second QH/QH2 reduction steps of the quinone reduction in the catalytic cavity of respiratory complex I. We find that pKa(QH-/QH2) is very high, above 20, while redox potential of QH/QH- is about −300mV. This means that the energy of a single protonation reaction of the reduced semiquinone QH- is sufficient to drive four protons across the membrane with a potential of 180mV. Based on these calculations, we propose a possible scheme of redox-linked proton pumping by complex I. The model explains how the energy of the protonation reaction can be divided equally between four pumping units of the pump, and how a single proton can drive translocation of four additional protons in multiple pumping blocks. The pumping reaction involves proton loading to multiple proton loading sites (PLS) in the "central axis" of Lys and Glu residues in the membrane arm of the enzyme and the displacement of the pumped protons by protonation of the "chemical" sites of the neighboring blocks; in this respect the reaction is similar to the scheme of pumping in cytochrome c oxidase in which a chemical proton coming to the binuclear center ejects the pumped proton from PLS. Within the proposed model, we discuss the catalytic cycle of the enzyme. We consider a possibility that a fifth energy-neutral proton in L(ND5)-subunit is cycling on one (P-) side of the membrane without crossing it, stabilizing the loaded (charged) state of the pump.

Single protonation of the reduced quinone drives four-proton pumping

1. FeS chain is in redox equilibrium with NADH pool, redox potential of N2 is −320mV, same as that of NADH.

In the reaction cycle, the quinone molecule migrates from the membrane into the binding chamber, diffuses up to N2 cluster, receives two electrons and migrates back – tail first,

from the narrow binding cavity to the membrane.[8, 18, 24, 26–29] Previously, based on our computer simulations of quinone entering the Q-binding site, we concluded that the reaction is bottlenecked by the binding (and unbinding) of the quinone.[30] This is due to a bottleneck at the entrance of the Q-binding cavity.[31] As NADH on the other side of the ET reaction chain does not have such constraints,[29] in the cycling enzyme the FeS chain is expected to be in redox equilibrium with NADH pool, with every other FeS cluster reduced,[32–34] including N2. (As FMN potential is somewhat higher than that of NADH, it is not expected to be reduced.) In such conditions, the redox potential of the N2 is lowered from −150 mV (at pH7)[35] to the potential of NADH,[36] i.e. around −320mV. Given that the potential of QH formation is some −300mV, there should be no problem of forming semiquinone.[36] This is in contrast to most previous studies of the quinone reduction where no such assumption was made[22] and the potential of N2 was assumed to be high, preventing easy semiquinone formation.[28] This model also suggests that the pH-dependence of N2 intrinsic potential[35] is not important for proton pumping by the enzyme.[37]

2. Redox chemistry at the Q-site. The pump is powered by QH/QH2 reduction.

The redox potential of Q/QH2 reduction (at pH7) is around +100mV, while redox potential of NADH oxidation is −320mV. Thus, upon transfer of electrons to quinone, the energy available is about 400mV per electron, which is sufficient to drive two protons across the membrane with a potential of 180–200mV. However, there are two electrons, and the energies available in Q/QH and QH/QH2 reactions are rather different,[36] being unequally divided between the two reactions. This is due to unstable nature of semi-quinone radical formed in the first reaction and its stabilization in the second reaction. From the data available, in aqueous media the redox potential of the first reduction Q/QH (pH7) is some −300mV (or somewhat lower) and that of the second QH/QH2 is +500mV(or somewhat higher), with pKa of Q- around 5, and QH- around 11. Electronic structure calculations and other analysis support this picture.[38] However, in the low-dielectric medium, the redox potentials and pKa values change dramatically, while the combined ET/PT energetics (i.e. Hydrogen Dissociation Energies, HDE) remain about the same.[38] This change and its consequences for the reaction in complex I are discussed next. Since the source of electrons, the reduced FeS chain, presumably has the potential around −300mV, and overall reaction is a combined ET/PT for which energetics HDE does not change, it is obvious that only the second reaction QH/QH2 can be the source of pumping energy. The QH/QH2 reaction energy 800mV is obviously sufficient to pump all *four* protons across the membrane with a potential of some 200mV. It is important to understand details of this reaction within the low dielectric medium of the protein.

3. pKa of the reduced quinone QH- in Q-cavity. The source of the pumping energy.

Quantitative estimate of pKa shift due to a change of solvation Born energy upon moving QH- from an aqueous high dielectric $\epsilon_w = 78$ to a protein low dielectric medium $\epsilon_p = 4$, assuming charge delocalization radius $a_0 = 2$Å, is as follows:

$$\Delta pK_a = \frac{1}{RT(\ln 10)} \frac{q^2}{2a_0}\left(\frac{1}{\epsilon_p} - \frac{1}{\epsilon_w}\right) \simeq 14 \quad (1)$$

which already indicates a significant shift of pKa of QH-. Given pKa (QH-) in water is in the range of 10 to 11,[39] the estimate suggests that in the protein medium pKa of QH- should be expected to be in the region above 20.

To further quantify ΔpK_a, we carried out DFT quantum chemistry calculations for 2,3-Dimethoxy-5,6-dimethylbenzene-1,4-diol, a model compound of ubiquinol where the polyisoprenoid side chain is replaced with a methyl group (denoted as QH2 as well), and its conjugate base (QH-) in both high dielectric ($\varepsilon_w = 78$) and low dielectric ($\varepsilon_p = 4$) conditions. The calculations were done using a method similar to that described in Ref.[40] by using Gaussian 16 program[41] with the B3LYP functional and 6–311++G(d,p) basis set. To accurately describe the changes in hydrogen bonds between the -OH group of QH2 and hydrating waters upon deprotonation, up to six water molecules were explicitly included in the quantum calculations. The SMD variant of the polarizable continuum model (PCM) was used to describe the dielectric effect. The Gibbs free energies of QH2 and QH- were calculated for their optimized geometries by including zero-point energies and thermal corrections based on their harmonic frequency calculations. The calculated pKa values of QH- at $\varepsilon_w = 78$ are 18.28 (with no explicit water), 15.95 (with 1 explicit water molecule), 12.94 (with 3 explicit water molecules), and 11.96 (with six water molecules), highlighting the importance of the hydrogen bond effect on the protonation/deprotonation of QH-/QH2. The calculated pKa of 11.96 with all essential hydrating waters included agrees well with the experimentally proposed value of around 11, confirming the validity of evaluating ΔpK_a by using DFT quantum calculations. The variation in DFT methods can only change the picture within one pKa unit.

At the low dielectric condition with $\varepsilon_p = 4$, the pKa (QH-/QH2) was calculated to be 26,15 (with 1 explicit water molecule), yielding ΔpK_a of 14.19. As seen, the calculated pKa values agree semi-quantitatively with the pure dielectric estimate, predicting pKa (QH-/QH2) above 20.

4. Redox potential of QH/QH- is around −300mV, same as reduced FeS chain.

By itself, the high pKa of QH- is not sufficient to be the source of energy of any following reaction. One needs to consider also the associated electron transfer energetics. As already indicated, the combined energy of ET/PT or BDE is about the same in any media, including protein (given not a strong polar nature of the quinones involved, their solvation does not change drastically). Hence, one can already conclude that the purely electronic energy should not contribute much to overall energetics of QH/QH2 reaction as the electrons are coming from a source of potential −300mV, i.e. that of reduced FeS chain. But it is interesting to consider explicitly the redox potential of QH/QH- reaction in Q-cavity. The estimate is obtained as follows.

In aqueous medium, the overall ET/PT redox potential of QH/QH2 pair is some +500mV; the contribution of the proton at pH7 is (pKa-pH)=11–7=4 pKa units, or 240mV. Hence, redox potential of QH/QH- is +260 mV. This is in high dielectric of water 80. In low dielectric of protein 4, the change of solvation energy is about the same as for protonated species, perhaps somewhat smaller as the charge is delocalized over larger area on the ion;

hence, the estimate should be somewhat smaller than in the above equation for $\Delta pKa = 14$ (i.e. change of solvation energy in pKa units). If one takes the lower conservative bound of 10pKa units, or 600mV, the redox potential comes about +260–600=−340mV. This is about the same as equilibrium redox potential of the reduced FeS chain and that of NADH, i.e. −320mV. Hence, the electron is transferred to QH to form QH- without losing or gaining any significant energy. Therefore, the remaining energy of the reaction is only related to proton transfer to QH- to form QH2. If proton is taken from the medium of pH7, this energy as we already know is pKa(QH-/QH2)-pH = 22–7=15 in pKa units, or 15×60=800mV, same as in BDE of QH2, as expected. This energy, 800mV, is sufficient to pump *four* protons across the membrane with potential of 180–200 mV.

5. Redox potential of Q/QH is around −300mV, same as reduced FeS chain, but the reaction can happen only as a concerted ET/PT process.

In water, pKa of Q-/QH protonation is about 5; this means that the redox potential of Q/Q- transition in water is Em(Q/QH)-(pKa-pH)*60mV=−300-(5–7)x60mV=−180mV. The change of solvation energy upon going from high- (water) to low-dielectric (protein) medium for redox pair Q/QH is expected to be about the same as for QH/QH2 species; i.e. around 10 to 12 pKa units. Hence, in low protein dielectric of 4, redox potential of Q/Q- transition is expected to be −180mV-720mV=−900mV, almost 600mV lower than the potential of FeS chain and that of N2. Hence, this transition has to be coupled to a proton transfer. For pKa (Q-/QH) in protein one expects a value of 5+12=17 or so; hence, the proton is adding energy of (pKa-pH)=17–7=10pKa units, or 600mV. This lowers the total energy of QH formation to the expected −300mV= (−900+600)mV. The proton for this reaction most likely comes from the Aps139-/His38+ pair, as many authors have proposed in the past.[1, 18, 28] Whether this reaction is true concerted PCET[28] or a sequential ET/PT[42] does not matter. Important for this discussion is that this reaction does not carry much energy change, and most surely is a slow (because of ET/PT coupling) process. But the formation of semiquinone is ensured by energetics and most likely was seen in the experiments of Ohnishi[43]. (We previously argued against the stable semiquinone species, and advocated a two-electron concerted reduction reaction[28] bypassing semiquinone formation; but that theory was based on the assumption of high potential of N2 (−150mV) usually assumed in the literature, unlike our current proposal of low potential of N2 of some −320mV.) Given that the following reaction of QH- formation is expected to be much faster than that of QH, this would make the semiquinone species only transient, explaining difficulty to observe it.[43]

6. Summary of Q/QH2 redox chemistry in Q-cavity of complex I.

Due to the bottleneck at the entrance of Q-cavity, the quinone binding is a slow and rate limiting step in the redox cycle, hence under normal cycling conditions the FeS chain is in redox equilibrium with NADH pool, hence the redox potential of the last N2 cluster is about the same as that of NADH, i.e. some −320mV. Given our calculations of pKa and redox potentials of the quinone in the low dielectric Q-cavity, we propose that the first reduction reaction of formation of semiquinone QH is a slow process, due to a very low potential of Q/Q- (some −900mV) and a need for a complementary proton, which presumably comes from Asp139-/His38+ pair; but the overall reaction of Q/QH transition is energy neutral, and

cannot provide any energy for pumping. Here, only one proton is needed. (This may explain the earlier results[21, 44] in which mutation of Tyr87 to Phe results in a drastic reduction of redox activity, but the *residual* activity was still showing almost normal pumping efficiency.)

The next redox step is a formation of QH- species, which does *not* need a proton, as the redox potential of QH/QH- is about the same as that of the reduced FeS chain, including N2. A stable QH- formed in this step has an exceptionally high pKa, above 20, and by our theoretical estimates is in the range of 22–26 in the Q-cavity. Thus, a single protonation of QH- carries energy (pKa-pH) of some 800mV, sufficient to pump *four* protons across the membrane with a potential of 180–200mV. Where this second proton is coming from appears to be a key question for the pumping mechanism.

7. The pump-driving proton for QH- protonation is coming from the E-channel in the Q-cavity.

We propose that this second, pump-driving proton is coming from the E-channel, when the reduced quinone QH- migrates down the Q-cavity to the lower binding site[29] near the entrance of the E-channel in the Q-cavity. (In one recent proposal,[15] *two* protons are proposed to be coming from E-channel.)

If so, the remaining questions concern the mechanism of delivering and dividing the available energy of protonation of QH- between the four pumped protons, and the actual mechanism of utilizing this energy for proton pumping. This will be addressed next.

Multi-Barrel Proton Pump Model

1. PT connectivity along the central axis.

The schematics of the proposed mechanism are shown in Fig. 1 and 2. The analysis is mostly based on *Thermus thermophilus* enzyme structure.

As shown in Fig. 1, the invariant E-channel formed by a chain of E- and D-residues extends from the middle part of the Q-cavity (H/E223, H/E225) to the middle part of the membrane arm of the enzyme (A/D72 on the TM2 of A/ND3-subunit), leading to the “central axis” of K- and E- residues of K/J and N, M, and L-subunits of the membrane arm of the enzyme. Our calculations[45] and recent structural data show water molecules that provide necessary connectivity between proton carrying groups present in that part of the enzyme.[13, 20, 46] The last residue of the E-channel on TM2 helix of A subunit is separated from the chain of central axis by a gap of some 15 angstroms, from the two E-residues of K-subunit and invariant Tyr59 on TM3 of J. No water molecules are seen in the gap in the recent structures. (However, some reports suggest that in the so-called “closed” state, the TM3 of J/ND6 subunit undergoes a rotation in such a way that a transient connectivity between the E-channel and K- and N- subunits is established[14–15] via J/Tyr59 and an assumed water chain; this was not observed in all enzymes, though. We do not consider here such a possibility in detail; however, an additional comment regarding this point will be provided in the end.)

The two E-residues of K- and one additional E-residue of N-subunit form the entrance to the central axis. The whole chain then can be described as follows:

$$(K_3^L K_2^L||K_1^L E_1^L)_L(.?. \\ )(E_2^M K_2^M||K_1^M E_1^M)_M ...(K_3^N K_2^N||K_1^N E_1^N)_N ...(EEE)_E QH - \quad (2)$$

where two subunits L- and N- contain three invariant Lys residues K1-K3, and the entry Glu residue, E1, with the structure (KK||KE); the M-subunit has the structure (EK||KE), and the E-channel is schematically shown as (EEE)_E. Also schematically, for the purpose of this discussion, we united the triad of Glu residues at the interface of N and K subunits as one residue E_1^N. At the entrance of the E-channel, the reduced QH- is docked, ready to receive a proton, as shown on the right in Fig. 2. All residues of E-channel are connected, as well as other residues not separated by any symbols, and assumed to allow proton transfer between them.

A key question about residues of the central axis is which residues are connected by proton transfer and which are disconnected. Structurally, one gap is suggested between the end of E-channel and the beginning of the central axis triad of Glu residues of K- and N-subunit interface. The gaps of this sort are described as (…) symbol on the scheme and shown as vertical dashed lines in Fig. 1. As seen from the scheme, we assume additional disconnections for PT between N- and M- subunits; however, a similar gap between M- and L- is shown as (.?.) indicating that it is likely that there is a continuous chain of residues that can conduct protons between K_1^L and K_2^M.

2. The pair Lys residues of the central axis are disconnected for proton transfer.

Our PT connectivity analysis[45] indicates that the central Lys residues in LMN-subunits are disconnected for proton transfer, which is indicated by symbol ||, as for example in $(K_3^L K_2^L||K_1^L E_1^L)$. Here two Lys' K1 || K2 are disconnected, while K3K2 are connected for proton transfer, according to our analysis. It should be mentioned that this is radically different from the recent proposal for PT connectivity along the whole central axis chain.[11, 46]

3. All residues of the central axis are strongly coupled by Coulomb interaction.

All residues of the central axis, connected or disconnected, are strongly coupled by the Coulomb interaction. The strength of the coupling is estimated to be about 250mV for pairs separated by 10 angstroms, or about 4 pKa units. All residues indicated on the scheme are separated by the distance of some 10 angstroms or so; therefore, assuming protein dielectric $\varepsilon_p = 4$, we find:

$$W_{ij} = \frac{q_i q_j}{R_{ij}} \frac{1}{\varepsilon_p} \approx 250mV\,.$$

This is a significant energy, which indicates a strong coupling. This energy is also an estimate of pKa shift of a given residue in the central axis by the charge of the neighboring

group, if the charge is present. This Coulomb interaction energy between the neighboring groups, the Coulomb Junctions (CJ), is playing a key role in the mechanism, as it gives rise to a strong correlation between the protonation states of the residues of the central axis in the neighboring pumping blocks, shown in Fig. 2.

4. Six pumping blocks of the multi-barrel pump.

The blocks that are disconnected for proton transfer, but connected by Coulomb Junctions, CJ's, are forming individual pumping blocks. If we assume the connectivity scheme shown above, i.e. L- and M- subunits are connected at interface, $||K_1^L E_1^L)(E_2^M K_2^M||$, and form one block, in which a proton can be transferred between K_1^L and K_2^M, there are six pumping blocks, including E-channel, with five Coulomb Junctions between them. Schematics of the pumping blocks is shown in Fig. 2. The E-block is directly coupled to QH-, which is bound at the entrance of the E-channel in the middle part of the Q-cavity. From the E-block a proton can be transferred to QH-, if energetics allows such a transfer.

5. Ground Protonation state of the central axis residues.

Using methods of pKa calculation developed in our previous work on cytochrome oxidase[47–48], and more recently on complex I,[49] we estimated that in the ground (resting) protonation state of the system all Lys residues on the left side of the block are protonated, while the Glu residues are mostly deprotonated or neutral as shown here:

$$(K_3^+K_2^0||K_1^+E_1^-)_L(E_2^0K_2^0||K_1^+E_1^-)_M...(K_3^+K_2^0||K_1^+E_1^-)_N...(EEE)_EQH- \quad (3)$$

This state is schematically shown in Fig. 2 upper panel as an initial state in the "Loading" transition.

The residues of the E-channel are all (or almost all) protonated and have high pKa values above 20. This estimate is corroborated by the data on the solvation enthalpy of carboxylate ions RCOO- in aqueous solutions of about 70–75kcal/mol,[50] and our estimate that in low dielectric protein medium of $\varepsilon_p = 4$, the change of solvation is about one quarter (due to Born factor $(\frac{1}{\varepsilon_p} - \frac{1}{\varepsilon_w})$) of the total solvation, i.e. roughly 72/4kca/mol $\approx 14pKa$ units. Given that pKa of carboxylates around 4 in water, possible slight variations in protein dielectric (it can locally be as low as 2), and the negative charge on the E_1^{N-}, all these factors bring the pKa of E-channel to above 20. It is yet possible that one or two residues of the E-channel is still deprotonated due to salt bridges, but it does not change the picture we develop next.

6. Loaded Protonation state of the central axis residues is formed by a strong Coulomb correlation.

The reduced semiquinone QH-, formed at the upper part of the Q-cavity, is moving around on the 10mks time scale in the binding cavity, binds at the second binding site near the entrance of E-channel, and can now get protonated by the reservoir of protons of the E-channel. Due to a strong Coulomb correlation of the central axis protons, the transfer of

a proton from the Glu residues of the E-channel will induce the concerted displacement of protons along the whole central axis, as shown in Fig. 2. This conclusion is based on the following considerations.

The collective pKa of the residues in the E-channel is above that of QH-, while both pKa's are above 20. Furthermore, we find that QH- cannot get protonated by the E-channel, unless a neighboring subunit $||K_1^{N+}E_1^{N-})$ moves its own proton closer to a nearest E-channel residue, to produce $||K_1^N E_1^N)(E^-...E)QH_2$ state and to neutralize an additional negative charge in the E-channel. The Coulomb energy of 250mV would make this transition possible. However, a PT transfer in only one subunit by itself is energetically also unfavorable, due to strong Coulombic interactions/correlations between protons in the low dielectric of the membrane part, and requires an *additional* PT in the adjacent block $(K_3^{N+}K_2^N||$ to make it $(K_3^N K_2^{N+}||$, etc. In other words, the transfer of a proton in the E-channel can only occur *together* with all other protons of the central axis, as shown in Fig. 2.

If protons in the loading stage move together, their proton-proton Coulombic energy does not change much, which is favorable for low energy protonation states. Such strongly correlated states were described in the context of complex I earlier.[49] As the Coulomb energy of proton-proton interaction does not change, as the protons are displaced in the direction of QH- along the central axis, as shown in Fig. 2, the increase of the energy of the loaded state is mostly due to a difference in pKa values of the residues of donors and acceptors (left and right sites in Fig. 2) in each block. As blocks are similar in structure, the energy associated with the transfer of protons will be equally divided between the blocks.

The resulting Loaded state of the pump is described now as:

$$(K_3^+K_2^+||K_1^0E_1^-)_L(E_2^0K_2^+||K_1^0E_1^0)_M...(K_3^0K_2^+||K_1^0E_1^0)_N...(E^-EE)_EQH_2 \quad (4)$$

It is seen, in Loading, as schematically shown in Fig. 2 upper panel, the protons are moved in a concerted fashion along the central axis from the Chemical (CHE) sites on the left to a Proton Loading Sites (PLS) on the right, with specifics given in the above equation. In order to stabilize the Loaded state, the last residue K_3^L has to be protonated; however, it is not yet clear which side of the membrane the last proton is coming from. Connectivity analysis indicates that the most likely coupling of K_3^L is to the positive P-side of the membrane, as shown in Fig. 1 and Fig. 2, lower panel. Due to the correlated nature of the formed state, the energy of the protonation of QH-, i.e. 800 mV is more or less equally divided between the pumping blocks and stored in each pumping block in the form of the difference in pKa values (about 3 pKa units, or in general greater than the PMF of the membrane, Δp_m) of the CHE and PLS sites. The loaded state (protonic excited state of the central axis), thus formed, carries all the energy of protonation transition QH-/QH2.

7. Proton pumping.

In each pumping block, the high pKa CHE site is connected to the negative N-side of the membrane, while the low pKa PLS site is connected to the positive P-side of the membrane (in the resting state, this connectivity maybe closed, but can be open due to local charge changes upon PLS Loading). In each pumping block the stored energy can spontaneously relax to the ground state by picking up a proton to an empty high pKa CHE site, which is connected only to the negative side of the membrane, and due to proton-proton repulsion via the Coulomb Junction will expel a proton from the PLS of a neighboring block, as shown schematically in Fig. 2, lower panel, to the positive side of the membrane. The strong correlation between the protons of the loaded state does not allow the protons to flow back in the same block, unless there is a membrane potential that exceeds the difference in the pKa values of CHE and PLS sites. Computer simulations of the pumping reaction (detailed report will be provided elsewhere) support the described picture. When the membrane potential or PMF is too high, i.e. $\Delta p_m > \Delta pKa(CHE/PLS)$, each pumping block leaks protons along the PT path from the P- side to N-side of the membrane, as expected.

Summary of the Pumping mechanism

Our analysis shows that a single protonation of the reduced semiquinone QH- can drive the four-proton pumping by complex I. The transduction of redox energy occurs in the formation of the (High-Energy) Loaded state of the protons in the central axis, which carries about all 800mV of available energy of protonation. The key feature of the Loaded state is a strong proton-proton correlation between the neighboring residues of the central axis, which imposes a concerted character of transfer of protons along the central axis, and which explains how total energy of the pumping is divided equally between the four pumping blocks. Such strongly-correlated protonic states in complex I were described previously.[49] The membrane arm of the enzyme consists of several pumping blocks; each block has a high pKa CHE protonation site and a low pKa PLS site. The Loading of the multi-unit pump occurs when the protons in the linear array of several blocks are transferred, in a concerted way, from the CHE site to PLS, a process driven by a single protonation of QH-. Within the pumping blocks CHE and PLS sites are connected for proton transfer, but the blocks are separated by gaps (no PT) which form Coulomb Junctions, i.e. Coulomb interaction of the neighboring protonation sites. CHE sites are connected to N-side of the membrane and PLS are connected to P-side, as shown in Fig. 1 and 2. The Pumping occurs when the high-energy Loaded state is spontaneously relaxes back to the ground sate by protonation of the empty high pKa CHE sites, which eject the protons from the PLS of the neighboring block across the Coulomb Junction. The mechanism in this respect is similar to that of Cytochrome c Oxidase with kinetic gating.[48] The necessary kinetic gating of the pump[24, 48] is ensured here by the correlated nature of the high-energy Loaded state. Both in Loading and Pumping transitions, no wave-propagation along the central axis envisioned in some models[16] appears to occur; at any rate, it carries no functional role in this model.

To stabilize the high-energy Loaded state, protonation of the last site Lys385 in L/ND5 is needed. This protonation appears to occur from the P-side of the membrane, and the connectivity of the pumping blocks indicates that there may be 5th proton cycling on the

same side of the membrane, not contributing to proton pumping but utilized instead for stabilization of the high-energy Loaded state. The alternative possibility would involve protonation of K385 from the N-side of the membrane and an assumption of connectivity of E-channel to the central axis residues due to TM3/ND6 rotation, as proposed recently.[14–15]

The need for stabilizing the Loaded state by a proton at Lys385 in L/ND5 may explain the results of mutation of that residue in ND5 affecting not only the pumping but also the redox chemistry (activity) of the enzyme.[51] Furthermore, the removal of two distal subunits of the enzyme ND5 and ND4 was reported to result in the proton pumping efficiency decrease by 50% (2H+/2e),[52] which is in agreement with the suggested scheme of distributed proton pumping blocks along the membrane arm of the enzyme, but contradicts a recent proposal of only one proton exit channel in ND5.[14, 46] On the other hand, the details of the proposed stabilization of the Loaded state in a half-truncated enzyme are not exactly clear at the moment, as the reliable prediction of PT pathways is still a serious computational challenge.

ACKNOWLEDGMENT

This work has been supported by the NIH research grant GM054052 (AAS).

DATA AVAILABILITY

The data that support the findings of this study are available from the corresponding author [aastuchebrukhov@ucdavis.edu] upon request.

Abbreviations:

CI	complex I
PLS	proton loading site
Thermus thermophilus	the numbering refers to bacterial enzyme

REFERENCES

1. Sazanov LA, A Giant Molecular Proton Pump: Structure and Mechanism of Respiratory Complex I. Nature Reviews Molecular Cell Biology 2015, 16, 375–388. [PubMed: 25991374]
2. Parey K; Wirth C; Vonck J; Zickermann V, Respiratory Complex I - Structure, Mechanism and Evolution. Curr Opin Struct Biol 2020, 63, 1–9. [PubMed: 32058886]
3. Gutierrez-Fernandez J; Kaszuba K; Minhas GS; Baradaran R; Tambalo M; Gallagher DT; Sazanov LA, Key Role of Quinone in the Mechanism of Respiratory Complex I. Nat Commun 2020, 11, 4135. [PubMed: 32811817]
4. Baradaran R; Berrisford JM; Minhas GS; Sazanov LA, Crystal Structure of the Entire Respiratory Complex I. Nature 2013, 494, 443–448. [PubMed: 23417064]
5. Fiedorczuk K; Letts JA; Degliesposti G; Kaszuba K; Skehel M; Sazanov LA, Atomic Structure of the Entire Mammalian Mitochondrial Complex I. Nature 2016, 538, 406–+. [PubMed: 27595392]
6. Letts JA; Fiedorczuk K; Degliesposti G; Skehel M; Sazanov LA, Structures of Respiratory Supercomplex I+Iii2 Reveal Functional and Conformational Crosstalk. Mol Cell 2019, 75, 1131–1146 e6. [PubMed: 31492636]
7. Zickermann V; Wirth C; Nasiri H; Siegmund K; Schwalbe H; Hunte C; Brandt U, Structural Biology. Mechanistic Insight from the Crystal Structure of Mitochondrial Complex I. Science 2015, 347, 44–9. [PubMed: 25554780]

8. Parey K; Haapanen O; Sharma V; Kofeler H; Zullig T; Prinz S; Siegmund K; Wittig I; Mills DJ; Vonck J; Kuhlbrandt W; Zickermann V, High-Resolution Cryo-Em Structures of Respiratory Complex I: Mechanism, Assembly, and Disease. Sci Adv 2019, 5, eaax9484. [PubMed: 31844670]
9. Agip AA; Blaza JN; Fedor JG; Hirst J, Mammalian Respiratory Complex I through the Lens of Cryo-Em. Annu Rev Biophys 2019, 48, 165–184. [PubMed: 30786232]
10. Guo R; Zong S; Wu M; Gu J; Yang M, Architecture of Human Mitochondrial Respiratory Megacomplex. Cell 2017, 170, 1247–1257 e12. [PubMed: 28844695]
11. Kampjut D; Sazanov LA, The Coupling Mechanism of Mammalian Respiratory Complex I. Science 2020, 370, 6516.
12. Bridges HR; Fedor JG; Blaza JN; Di Luca A; Jussupow A; Jarman OD; Wright JJ; Agip AA; Gamiz-Hernandez AP; Roessler MM; Kaila VRI; Hirst J, Structure of Inhibitor-Bound Mammalian Complex I. Nat Commun 2020, 11, 5261. [PubMed: 33067417]
13. Grba DN; Hirst J, Mitochondrial Complex I Structure Reveals Ordered Water Molecules for Catalysis and Proton Translocation. Nat Struct Mol Biol 2020, 27, 892–900. [PubMed: 32747785]
14. Kampjut D; Sazanov LA, Structure of Respiratory Complex I - an Emerging Blueprint for the Mechanism. Curr Opin Struct Biol 2022, 74, 102350. [PubMed: 35316665]
15. Vercellino I; Sazanov LA, The Assembly, Regulation and Function of the Mitochondrial Respiratory Chain. Nat Rev Mol Cell Biol 2022, 23, 141–161. [PubMed: 34621061]
16. Kaila VRI, Resolving Chemical Dynamics in Biological Energy Conversion: Long-Range Proton-Coupled Electron Transfer in Respiratory Complex I. Acc Chem Res 2021, 54, 4462–4473. [PubMed: 34894649]
17. Kampjut D; Sazanov LA, Structure and Mechanism of Mitochondrial Proton-Translocating Transhydrogenase. Nature 2019, 573, 291–295. [PubMed: 31462775]
18. Kaila VRI, Long-Range Proton-Coupled Electron Transfer in Biological Energy Conversion: Towards Mechanistic Understanding of Respiratory Complex I. J R Soc Interface 2018, 15, Article ID:20170916.
19. Kaila VR; Wikstrom M; Hummer G, Electrostatics, Hydration, and Proton Transfer Dynamics in the Membrane Domain of Respiratory Complex I. Proc Natl Acad Sci U S A 2014, 111, 6988–93. [PubMed: 24778264]
20. Gu J; Liu T; Guo R; Zhang L; Yang M, The Coupling Mechanism of Mammalian Mitochondrial Complex I. Nat Struct Mol Biol 2022, 29, 172–182. [PubMed: 35145322]
21. Tocilescu MA; Zickermann V; Zwicker K; Brandt U, Quinone Binding and Reduction by Respiratory Complex I. Biochim Biophys Acta 2010, 1797, 1883–90. [PubMed: 20493164]
22. Hayashi T; Stuchebrukhov AA, Electron Tunneling in Respiratory Complex I. Proc Natl Acad Sci U S A 2010, 107, 19157–19162. [PubMed: 20974925]
23. Cabrera-Orefice A; Yoga EG; Wirth C; Siegmund K; Zwicker K; Guerrero-Castillo S; Zickermann V; Hunte C; Brandt U, Locking Loop Movement in the Ubiquinone Pocket of Complex I Disengages the Proton Pumps. Nat Commun 2018, 9, 4500. [PubMed: 30374105]
24. Stuchebrukhov AA, Redox-Driven Proton Pumps of the Respiratory Chain. Biophys J 2018, 115, 830–840. [PubMed: 30119834]
25. Stuchebrukhov AA, Kinetics and Efficiency of Energy-Transducing Enzymes. J Phys Chem B 2019, 123, 9456–9465. [PubMed: 31557438]
26. Warnau J; Sharma V; Gamiz-Hernandez AP; Di Luca A; Haapanen O; Vattulainen I; Wikstrom M; Hummer G; Kaila VRI, Redox-Coupled Quinone Dynamics in the Respiratory Complex I. Proc Natl Acad Sci U S A 2018, 115, E8413–E8420. [PubMed: 30120126]
27. Wikstrom M; Sharma V; Kaila VR; Hosler JP; Hummer G, New Perspectives on Proton Pumping in Cellular Respiration. Chemical Reviews 2015, 115, 2196–221. [PubMed: 25694135]
28. Hagras MA; Stuchebrukhov AA, Concerted Two-Electron Reduction of Ubiquinone in Respiratory Complex I. J Phys Chem B 2019, 123, 5265–5273. [PubMed: 31141364]
29. Fedor JG; Jones AJY; Di Luca A; Kaila VRI; Hirst J, Correlating Kinetic and Structural Data on Ubiquinone Binding and Reduction by Respiratory Complex I. Proc Natl Acad Sci U S A 2017, 114, 12737–12742. [PubMed: 29133414]

30. Wang P; Dhananjayan N; Hagras M; Stuchebrukhov AA, Respiratory Complex I: Bottleneck at the Entrance of Quinone Site Requires Conformational Change for Its Opening. BBA - Bioenergetics 2021, 1862, 148326. [PubMed: 33045211]

31. Dhananjayan N; Wang P; Leontyev I; Stuchebrukhov AA, Quinone Binding in Respiratory Complex I: Going through the Eye of a Needle. The Squeeze-in Mechanism of Passing the Narrow Entrance of the Quinone Site. Photochem Photobiol Sci 2021, 21, 1–12. [PubMed: 34813075]

32. Bridges HR; Bill E; Hirst J, Mossbauer Spectroscopy on Respiratory Complex I: The Iron-Sulfur Cluster Ensemble in the Nadh-Reduced Enzyme Is Partially Oxidized. Biochemistry 2012, 51, 149–58. [PubMed: 22122402]

33. Hirst J; Roessler MM, Energy Conversion, Redox Catalysis and Generation of Reactive Oxygen Species by Respiratory Complex I. Biochim Biophys Acta 2016, 1857, 872–83. [PubMed: 26721206]

34. Medvedev ES; Couch VA; Stuchebrukhov AA, Determination of the Intrinsic Redox Potentials of Fes Centers of Respiratory Complex I from Experimental Titration Curves. Biochim Biophys Acta 2010, 1797, 1665–71. [PubMed: 20513348]

35. Le Breton N; Wright JJ; Jones AJY; Salvadori E; Bridges HR; Hirst J; Roessler MM, Using Hyperfine Electron Paramagnetic Resonance Spectroscopy to Define the Proton-Coupled Electron Transfer Reaction at Fe-S Cluster N2 in Respiratory Complex I. J Am Chem Soc 2017, 139, 16319–16326. [PubMed: 29039928]

36. Verkhovskaya M; Wikström M, Oxidoreduction Properties of Bound Ubiquinone in Complex I from Escherichia Coli. Biochim Biophys Acta 2014, 1837, 246–250. [PubMed: 24216024]

37. Zwicker K; Galkin A; Drose S; Grgic L; Kerscher S; Brandt U, The Redox-Bohr Group Associated with Iron-Sulfur Cluster N2 of Complex I. Journal of Biological Chemistry 2006, 281, 23013–23017. [PubMed: 16760472]

38. Zhu Z; Gunner MR, Energetics of Quinone-Dependent Electron and Proton Transfers in Rhodobacter Sphaeroides Photosynthetic Reaction Centers. Biochemistry 2005, 44, 82–96. [PubMed: 15628848]

39. Hasegawa R; Saito K; Takaoka T; Ishikita H, Pk a of Ubiquinone, Menaquinone, Phylloquinone, Plastoquinone, and Rhodoquinone in Aqueous Solution. Photosynth Res 2017, 133, 297–304. [PubMed: 28405861]

40. Thapa B; Schlegel HB, Improved Pka Prediction of Substituted Alcohols, Phenols, and Hydroperoxides in Aqueous Medium Using Density Functional Theory and a Cluster-Continuum Solvation Model. J Phys Chem A 2017, 121, 4698–4706. [PubMed: 28564543]

41. Frisch MJT, G. W.; Schlegel HB; Scuseria GE; Robb MA; Cheeseman JR; Scalmani G; Barone V; Petersson GA; et al. Gaussian 16, Revision C.01, Gaussian, Inc.: Wallingford, CT, USA, 2016.

42. Hammes-Schiffer S; Stuchebrukhov AA, Theory of Coupled Electron and Proton Transfer Reactions. Chemical Reviews 2010, 110, 6939–6960. [PubMed: 21049940]

43. Ohnishi T; Ohnishi ST; Salerno JC, Five Decades of Research on Mitochondrial NADH-Quinone Oxidoreductase (Complex I). Biol Chem 2018, 399, 1249–1264. [PubMed: 30243012]

44. Tocilescu MA; Fendel U; Zwicker K; Drose S; Kerscher S; Brandt U, The Role of a Conserved Tyrosine in the 49-Kda Subunit of Complex I for Ubiquinone Binding and Reduction. Biochim Biophys Acta 2010, 1797, 625–32. [PubMed: 20117074]

45. Wang P; Stuchebrukhov A, Water Channels in Respiratory Complex I 2022, to be submitted.

46. Parey K; Lasham J; Mills DJ; Djurabekova A; Haapanen O; Yoga EG; Xie H; Kuhlbrandt W; Sharma V; Vonck J; Zickermann V, High-Resolution Structure and Dynamics of Mitochondrial Complex I-Insights into the Proton Pumping Mechanism. Sci Adv 2021, 7, eabj3221. [PubMed: 34767441]

47. Quenneville J; Popovic DM; Stuchebrukhov AA, Combined Dft and Electrostatics Study of the Proton Pumping Mechanism in Cytochrome C Oxidase. Biochim Biophys Acta 2006, 1757, 1035–46. [PubMed: 16458251]

48. Popovic DM; Stuchebrukhov AA, Proton Pumping Mechanism and Catalytic Cycle of Cytochrome C Oxidase: Coulomb Pump Model with Kinetic Gating. FEBS Lett 2004, 566, 126–130. [PubMed: 15147881]

49. Couch V; Stuchebrukhov A, Proteins as Strongly Correlated Protonic Systems. FEBS Lett 2012, 586, 519–25; DOI: 10.1016/j.febslet.2011.09.036. [PubMed: 21985970]

50. Wilson B; Georgiadis R; Bartmess JE, Enthalpies of Solvation of Ions. Caboxylic Acids. J Am Chem Soc 2012, 113, 1762.

51. Nakamaru-Ogiso E; Kao MC; Chen H; Sinha SC; Yagi T; Ohnishi T, The Membrane Subunit Nuol(Nd5) Is Involved in the Indirect Proton Pumping Mechanism of Escherichia Coli Complex I. J Biol Chem 2010, 285, 39070–8. [PubMed: 20826797]

52. Drose S; Krack S; Sokolova L; Zwicker K; Barth HD; Morgner N; Heide H; Steger M; Nubel E; Zickermann V; Kerscher S; Brutschy B; Radermacher M; Brandt U, Functional Dissection of the Proton Pumping Modules of Mitochondrial Complex I. PLoS Biol 2011, 9, e1001128. [PubMed: 21886480]

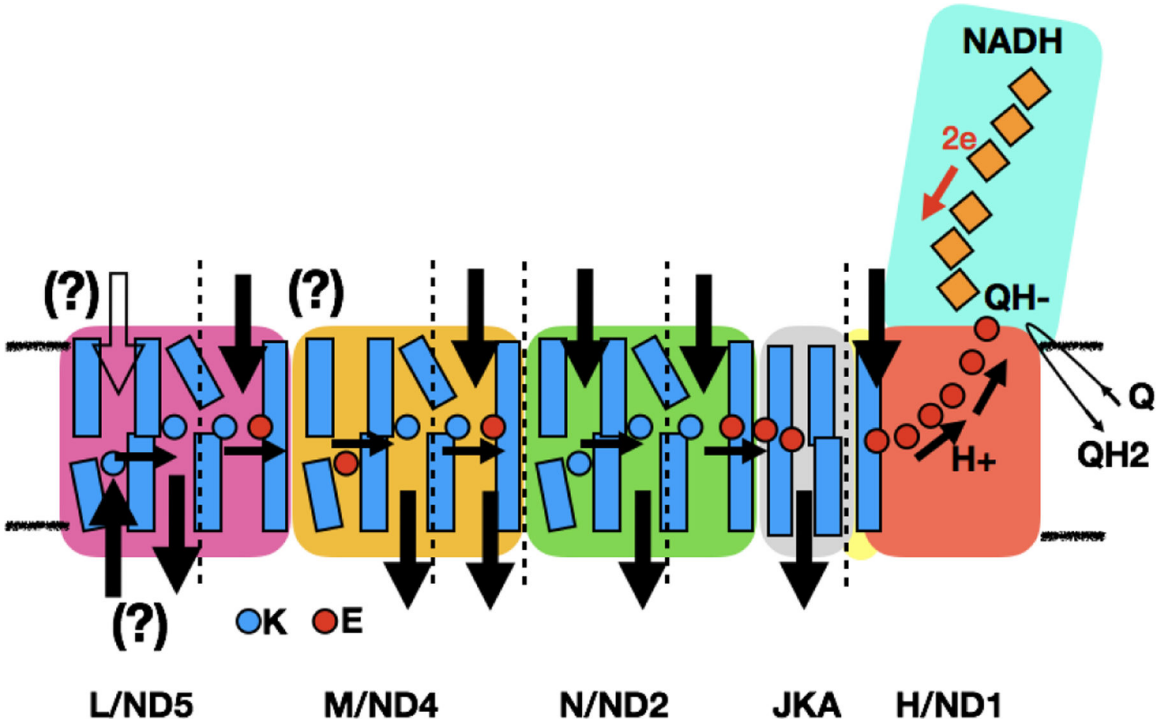

Fig. 1.

Schematics of complex I structure and proposed pumping scheme. Residues of the central axis shown left to right (numbering from *Thermus thermophilus*): L/K385, K329, K216, E132; M/E377, K325, K204, E123; N/K345, K216, K186, E112; K/E32, E67; E-Channel: A/D72; H/E130…E223, E225. The key residues were identified already in the initial structure[1, 4]; however, the PT "wiring" of these residues remains unclear. Proposed disconnections along the central axis are shown as dashed vertical lines. The "chemical" protons are coming from the N-side (top) and expel the pump protons from PLS's to P-side (bottom) of the membrane. The question marks indicate additional uncertainties including a possible 5th proton pumping in L-subunit.

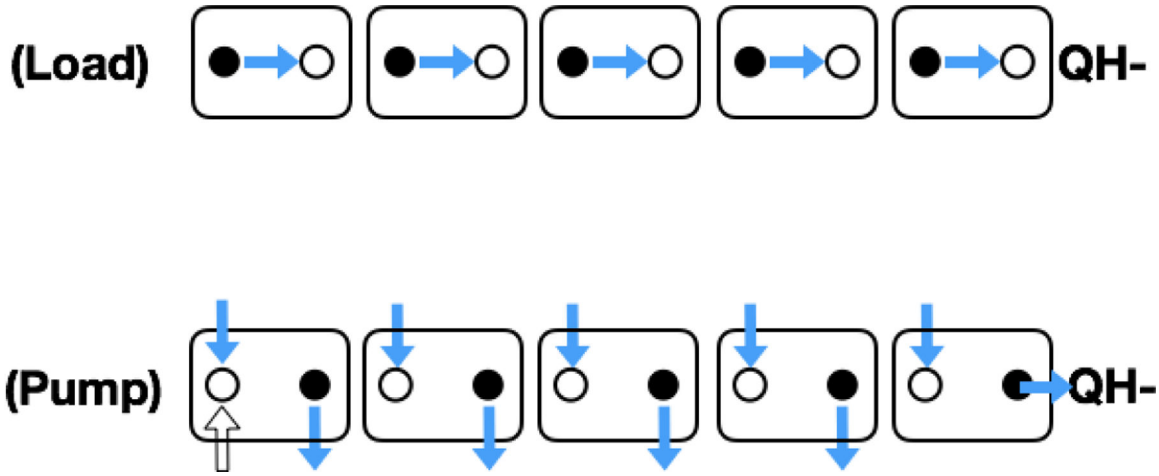

Fig. 2.

Schematics of multi-barrel proton pump. The pump consists of several similar basic pump units (not necessarily identical to antiporter-like subunits) and is powered by a single protonation of the reduced quinone QH- in the Q-cavity of the enzyme. In Loading, the protonation of QH- drives a concerted transfer of protons to units' PLS (the rightmost site of each unit) in each of the pump units along the axis of the enzyme, thereby pumping energy is stored and equally divided between the pumping blocks. In Pumping, the incoming "chemical" protons, coming to the vacated sites of the unit, and acting as "hammers", displace the protons from the PLS of each pumping unit.